Evaluating Discrete Time Methods for Subgrouping Continuous Processes

Jonathan J. Park, Zachary Fisher, Sy-Miin Chow, and Peter C. M. Molenaar

Department of Human Development and Family Studies, The Pennsylvania State University

Abstract

Rapid developments over the last several decades have brought increased focus and attention to the role of time scales and heterogeneity in the modeling of human processes. To address these emerging questions, subgrouping methods developed in the discrete-time framework—such as the vector autoregression (VAR)—have undergone widespread development to identify shared nomothetic trends from idiographic modeling results. Given the dependence of VAR-based parameters on the measurement intervals of the data, we sought to clarify the strengths and limitations of these methods in recovering subgroup dynamics under different measurement intervals. Building on the work of Molenaar and collaborators for subgrouping individual time-series by means of the subgrouped chain graphical VAR (scgVAR) and the subgrouping option in the group iterative multiple model estimation (S-GIMME), we present results from a Monte Carlo study aimed at addressing the implications of identifying subgroups using these discrete-time methods when applied to continuous-time data. Results indicate that discrete-time subgrouping methods perform well at recovering true subgroups when the measurement intervals are large enough to capture the full range of a system's dynamics, either via lagged or contemporaneous effects. Further implications and limitations are discussed therein.

Keywords: Dynamic Network Modeling, Vector Autoregression,

Continuous-Time Word Count: 4656

Introduction

In 2004, Peter Molenaar published a manifesto calling for a return of the person to the scientific study of psychology (Molenaar, 2004). Slowly but surely, the scientific

study of psychology has seen steady increases in the application of idiographic methods for studying person-specific processes in fields ranging from the analysis of fMRI data (Gates & Molenaar, 2012) to affective dynamics (De Vos et al., 2017; Wright et al., 2019). This has led to a general increase in our understanding of individual psychological and behavioral processes. However, as the late physicist John Archibald Wheeler once remarked, "[...] As our island of knowledge grows, so does the shore of our ignorance." (Horgan, 1992). Appropriately, these advances in understanding have been accompanied by a commensurate increase in questions that must be addressed.

For instance, while great progress has been made in developing methods that account for, and characterize, between-person heterogeneity in dynamic processes, less attention has been devoted to understanding how sensitive these methods are to violations of their assumptions. Importantly, while it is increasingly recognized that many processes of interest to psychologists unfold continuously over time, popular approaches for clustering individuals based on their time-series dynamics assume the sampling rate of the underlying process is well-specified. In this paper, we introduce continuous-time processes and two popular discrete-time modeling approaches that account for betweenperson heterogeneity at the process level. We will then examine how these dynamic network models and their subgrouping algorithms perform when applied to continuous processes at varying intervals of time, Δt . Specifically, we compare two popular methods, subgrouped chain graphical VAR (scgVAR; Park et al., 2022) and subgrouping with group iterative multiple model estimation (S-GIMME; Gates et al., 2017) and discuss the influence of varying sampling intervals on subgroup and parameter recovery. Finally, we offer some practical insights on key considerations for subgrouping with real-world dynamic network data.

Continuous Time Processes

To begin, we discuss the nature of modeling individuals over time. Processes can be thought of as unfolding continuously over time and relating to one another with varying strengths as a function of that time (Voelkle et al., 2012). Continuously evolving processes may be described as a set of differential equations that describe how change in one variable may affect change of another variable and can be expressed in the following general form:

$$d\eta(t) = [\mathbf{b} + \mathbf{A}\eta(t)] dt + \mathbf{G}d\mathbf{W}(t)$$
 (1)

where $d\eta$ is a p-variate set of differentials (changes) in a vector of latent variables, $\eta(t)$, \mathbf{A} is a $p \times p$ drift matrix which describes how changes in the values of η at time relate to itself and other variables, \mathbf{b} is a vector of intercepts. $\mathbf{W}(t)$ is a vector of process noises (specifically, standard Wiener processes) whose changes between any two time points, $d\mathbf{W}(t)$, are assumed to be normally distributed with zero means and variance-covariances

This work was supported by the Intensive Longitudinal Health Behavior Cooperative Agreement Program funded by the National Institutes of Health under Award Number U24AA027684 and the National Science Foundation grant IGE-1806874 alongside grants UH3 OD023389, 5 R01 HD097189-04, U2C OD023375, and 5 UL1TR002014-06.

that depend on G, the diffusion matrix, and the time interval between two time points, Δt . (Arnold, 1974; Voelkle et al., 2012).

The strengths of formulating change processes within a continuous-time (CT) framework are numerous (Chow et al., 2022; Ryan & Hamaker, 2022). In contrast to modeling variables in discrete-time (DT), CT models are able to handle irregularly spaced data and are not particularly sensitive to the sampling rate of the data (Gollob & Reichardt, 1987; Ryan & Hamaker, 2022). That said, the popularity of DT models far eclipses that of CT models in the social and behavioral sciences for a few practical reasons: measurements are typically taken in discrete time intervals (e.g., every day, week, month, etc.), DT models are typically simpler to interpret, and are more familiar to behavioral scientists (Ryan & Hamaker, 2022). The historical popularity of DT approaches also means CT-analogues of many popular DT modeling approaches have yet to be developed. For this reason, it is important to better understand the implications of applying DT models to CT processes.

Modeling in Discrete Time

The Vector Autoregressive (VAR) Model. The VAR model is a common approach for modeling multivariate time series. The parameters of the VAR can be used to characterize the dynamics of a system of variables at a given, discrete lag (Lütkepohl, 2005) with VAR models quickly becoming an invaluable methodological tool for understanding person-specific processes. Importantly, VAR models have proved invaluable for studying individuals in dynamic networks large enough to include many theoretically-relevant constructs (~5 to 30 variables; Bringmann et al., 2018; Epskamp, Waldorp, et al., 2018; Park et al., 2021). We describe the standard VAR(1) model of centered variables as:

$$\boldsymbol{\eta}_t = \boldsymbol{\Phi}_1^* \boldsymbol{\eta}_{t-1} + \boldsymbol{\zeta}_t^*. \tag{2}$$

where Φ_1^* is a p-dimensional matrix of auto- and cross-regression coefficients capturing the lagged effects of the observed variables, and ζ_t^* is the p-variate vector of process noises which are assumed to be independent and normally distributed; $\zeta_t^* \sim N(0, \Psi^*)$.

When fitting DT VAR models to continuous processes, some information relating to the dynamics may not be captured depending on the size of the sampling interval (i.e., Δt). In the following section, we discuss the relations between the DT VAR with their CT counterparts to provide an intuition as to *where* this information manifests in the DT VAR.

Relating Continuous and Discrete Time. Several authors (e.g., Voelkle et al., 2012) have noted that analytic solutions exist which map out values of η_t at any arbitrary timepoint based on Eq. 1. The set of exact transformations described below can transform the elements from the general stochastic differential equation in Eq. 1 into the equivalent forms of the VAR model in Eq. 2 at a given Δt (see Eqs 7-11; Voelkle et al., 2012):

$$\mathbf{\Phi}^*(\Delta t) = e^{\mathbf{A}\Delta t} \tag{3}$$

$$\mathbf{\Psi}^*(\Delta t) = \operatorname{irow}\{\mathbf{A}_{\#}^{-1}[e^{\mathbf{A}_{\#}\Delta t} - \mathbf{I}]\operatorname{row}(\mathbf{Q})\}$$
(4)

where $A_{\#} = A \otimes I + I \otimes A$; row(.) is a row operator which transforms a matrix row-wise into a column vector and irow(.) is the reverse operation turning a column vector into a matrix, \mathbf{Q} is the continuous-time error covariance matrix also known as the diffusion

matrix (Arnold, 1974; Voelkle et al., 2012). One critical feature of the CT VAR is that the sampling interval, Δt , is explicitly encoded into both Φ^* and Ψ^* , thus allowing parameters in the CT VAR to be uniquely defined regardless of the values of Δt . In contrast, the DT VAR model requires the observed data to be equally spaced to obtain Φ^* and Ψ^* as constant (Δt -invariant) values. These relations are summarized in part in Figure 1 and show how parameters from a CT model may be transformed and manifest at different sampling intervals (i.e., $\Delta t = 1$ or 10).

Notice the current set of scores in Equation 2 depends only on the previous time point. Thus, any lagged effects among variables that occur faster than the sampling rate will be captured in the process-noise covariance matrix, Ψ^* , as contemporaneous effects. The contemporaneous effects can be deduced explicitly using variants of the VAR model, such as the graphical VAR (gVAR; Epskamp, Waldorp, et al., 2018) for non-directed effects and the structural VAR (sVAR; Lütkepohl, 2005) for directed contemporaneous effects. That is, these variants of the standard VAR may be used to explicitly model dynamics which occur faster than a given measurement interval.

While the gVAR and sVAR models may—to an extent—be able to compensate for a mismatch between the underlying process and the sampling interval by modeling contemporaneous effects, some limitations remain. For instance, our discussions thus far have only discussed fitting a single model to a single subject. Some issues arise when faced with modeling multiple subjects such as how one deals with within-sample heterogeneity. Following, we discuss these challenges and some approaches that have been developed for tackling these issues.

Clustering of Discrete Time Dynamic Networks

The question as to how one may reconcile person- and group-level inferences has risen in tandem with the person-specific paradigm. Myriad methodologies exist for balancing individual- and group-specific inference under an umbrella term referred to as "idio-thetic" methods (Beck & Jackson, 2020). While a full discussion could be had on the full breadth of these methods, we instead focus on two methods which identify group-, subgroup-, and individual-level trends in novel ways and have been inspired—if not directly influenced—by Molenaar's work. Here, we outline these two approaches for clustering dynamic networks: the subgrouped chain graphical VAR (Park et al., 2022, scgVAR,) and the subgrouping option in the group iterative multiple model estimation (S-GIMME; Gates et al., 2017) procedure. In doing so, we will introduce the larger modeling frameworks these approaches are built on, graphical VAR and GIMME, respectively. Lastly, we will discuss important ways these approaches differ in relation to recovering contemporaneous relations.

Subgroup Chained Graphical VAR

The scgVAR (Park et al., 2022) is an idio-thetic method that serves to find homogeneous subgroups within the framework of the graphical VAR model. As the scgVAR approach utilizes the gVAR modeling framework it is useful to first review gVAR specification and estimation.

gVAR. In the gVAR approach, parameters from the standard VAR model are transformed onto a correlation scale (Epskamp, van Borkulo, et al., 2018; Park et al., 2021; Wild et al., 2010). These transformed parameters are referred to as the partial contemporaneous correlations (PCCs) and partial directed correlations (PDCs) obtained as:

$$PCC_{(\eta_m,\eta_n)} = -\frac{\kappa_{mn}}{\sqrt{k_{mm}\kappa_{nn}}} \tag{5}$$

where κ_{nn} and κ_{mm} are diagonal elements and κ_{mn} are off-diagonal elements from the precision matrix of the VAR where $\mathbf{K} = \mathbf{\Psi}^{*-1}$. The resulting **PCC** matrix is then a partial correlation matrix representing the contemporaneous relations between the m and n^{th} variables after conditioning on all other variables.

$$PDC_{(\eta_m,\eta_n)} = \frac{\phi_{mn}^*}{\sqrt{\psi_{mm}^* \kappa_{nn} + \phi_{mn}^{*2}}}$$
 (6) where ϕ_{mn}^* indicates the m^{th} row and n^{th} column element of Φ^* , ψ_{mm}^* represents a diag-

where ϕ_{mn}^* indicates the m^{th} row and n^{th} column element of Φ^* , ψ_{mm}^* represents a diagonal element of the covariance matrix of the VAR, Ψ^* . Here, the **PDC** matrix indicates the lagged relations between the m and n^{th} variables after conditioning on all others. One common approach for estimating a gVAR is with the least absolute shrinkage and selection operator (LASSO; Rothman et al., 2010; Tibshirani, 1996) but other estimation routines may also be used. Regularization methods such as the LASSO are favorable for estimating these effects as they produce sparse networks (Epskamp, Waldorp, et al., 2018). Notably, the contemporaneous effects as conveyed through the PCCs are agnostic regarding the *direction* of effects (Epskamp, Waldorp, et al., 2018).

sgcVAR. The subgrouping extension of the scgVAR algorithm begins by fitting graphical VAR models to all N subjects in a given sample. Following this, a similarity matrix is constructed, \mathbf{D} where any element, d_{pq} indicates the number of dynamic parameters the p and q^{th} subjects share in common with one another. Here, commonality is defined as any instance where a pair of subjects both share a non-zero parameter of similar polarity. For instance, if $\phi_{1,2}=0.3$ for the p^{th} subject and $phi_{1,2}=-0.3$ for the q^{th} subject then our algorithm would classify them as separate due to the difference in polarity (i.e., 0.3 vs -0.3). A community detection approach–WalkTrap (Pons & Latapy, 2005)–is then applied to \mathbf{D} to identify subgroups of individuals whose dynamics are most similar to one another. Finally, a group-level model is fitted to the sample by chaining the timeseries together and subgroup-level models are estimated by chaining together subjects assigned to the same communities.

Subgrouping Group Iterative Multiple Model Estimation

The S-GIMME algorithm (Gates et al., 2017) is an extension of the GIMME ecosystem designed to provide functionality for clustering individuals based on similarities and differences in their dynamic process. and is foundationally built upon the structural VAR model. We first introduce the structural VAR, then discuss the broader GIMME algorithm before finishing with developments specific to subgrouping individuals.

sVAR. While the scgVAR approach is built upon the graphical VAR model, GIMME and S-GIMME are based on the structural-VAR (Lütkepohl, 2005). The sVAR model provides an alternative method for explicitly modeling directional associations in the contemporaneous space and is parameterized as follows:

$$\eta_t = \mathbf{\Phi}_0 \eta_t + \mathbf{\Phi}_1 \eta_{t-1} + \zeta_t \tag{7}$$

where Φ_0 is the $p \times p$ regression matrix containing the contemporaneous effects with 0's along the diagonal, Φ_1 is the $p \times p$ regression matrix of lagged effects, and ζ is the p variate residual vector. The sVAR's Φ_0 matrix encodes the contemporaneous directional effect of each variable on one another. Notably, the Φ_1^* from Eq. 2 also differs from the Φ_1 in Eq. 7. Specifically, Φ_1^* pertains to the lagged coefficients matrix of the standard VAR model and Φ_1 pertains to the lagged coefficients matrix of the structural VAR, which capture lingering associations among the variables that are not accounted for by the contemporaneous effects in Φ_0 . In practice, the values contained in both matrices will differ in the presence of directed contemporaneous relations.

As written, the structural parameters of the sVAR are not identified, and a number of approaches for identification have been proposed in the literature. For example, a VAR(1) may be transformed to an sVAR(1) by means of Cholesky decomposition on the residual covariance matrix (Lütkepohl, 2005; Molenaar, 2017); however, this approach has been criticized due to the effect that ordering may have on the recovery of directed contemporaneous effects. For example, the first variable may have contemporaneous effects on all other *p*-variables but the second variable may only influence the variables inputted after and not the first variable. Thus, the decision on how one orders the variables in the analysis may have an impact on the recovered directionality of contemporaneous effects (Lütkepohl, 2005). In some instances, theory may be used to guide the ordering of the variables; however, in higher dimensional dynamic networks, this may not be feasible. Another approach for dealing with the identification issue for sVAR models is the GIMME algorithm and is discussed below.

GIMME. The sVAR implementation in GIMME and S-GIMME resolves the identifiability issue raised previously by relying on a diagonal structure imposed on the process noise covariance matrix, $\text{Cov}(\zeta_t)$, as well as unique information conveyed by each process's autoregressive parameter, to identify the reciprocal effects (i.e., those of $\eta_{k,it} \to \eta_{k',it}$ and $\eta_{k',it} \to \eta_{k,it}$; $k \neq k'$) between any two variables in η_{it} that dissipate at a faster rate than those reflected at $\Delta t = 1$ (Gates et al., 2010).

The GIMME algorithm operates by means of specifying a null sVAR model to all individuals in a given dataset. As noted above, this null model is one in which all autoregressive effects and all diagonal elements of the residual covariance matrix are freed for estimation for all subjects. Following this, modification indices are assessed across all individuals and parameters are freed for estimation if they would improve model fit for a user-defined percentage of individuals until no paths in either Φ_0 or Φ_1 would improve the model fit for the specified percentage of individuals (Gates & Molenaar, 2012). Following this step, paths which were added in previous steps that are no longer statistically significant for a majority of individuals are pruned from the group-level model. Then, GIMME concludes with individual model estimation using the same iterative procedure of assessing person-specific modification indices.

S-GIMME. The Subgrouping Group Iterative Multiple Model Estimation (S-GIMME; Gates et al., 2017) algorithm is an idio-thetic method built on the GIMME framework to further identify subgroup-level information along with the group- and individual-level processes via an iterative procedure and community detection (see Gates et al., 2017, Figure 3). Simply, S-GIMME identifies group-level paths which improve model fit for a majority of individuals discussed in the previous section. Group-level paths—in the case

Table 1 Transformations relating parameters of the CT VAR to the DT VAR, sVAR, and gVAR

	, , , ,
$CT VAR \rightarrow DT VAR$ at fixed equal A	
$oldsymbol{A} o oldsymbol{\Phi}^*(\Delta t)$	$\mathbf{\Phi}^*(\Delta t) = e^{\mathbf{A}\Delta t}$
$\mathbf{Q} o \mathbf{\Psi}^*(\Delta t)$	$\mathbf{\Psi}^*(\Delta t) = \operatorname{irow}\{\mathbf{A}_{\#}^{-1} \left[e^{\mathbf{A}_{\#}\Delta t} - \mathbf{I} \right] \operatorname{row}(\mathbf{Q}) \}$
sVAR \rightarrow DT VAR with known Δt	
$oldsymbol{\Phi}_0 \ \& \ oldsymbol{\Phi}_1 ightarrow oldsymbol{\Phi}_1^*$	$\mathbf{\Phi}_1^* = (\mathbf{I} - \mathbf{\Phi}_0)^{-1} \mathbf{\Phi}_1$
-	- '
$oldsymbol{\Phi}_0 \ \& \ oldsymbol{\Psi} ightarrow oldsymbol{\Psi}^*$	$\mathbf{\Psi}^{*}=\left(\mathbf{I}-\mathbf{\Phi}_{0} ight)\mathbf{\Psi}\left(\mathbf{I}-\mathbf{\Phi}_{0} ight)^{\prime}$
	$\mathbf{\Psi}^* = (\mathbf{I} - \mathbf{\Phi}_0) \mathbf{\Psi} (\mathbf{I} - \mathbf{\Phi}_0)'$
DT VAR \rightarrow gVAR with known Δt	
	$\mathbf{\Psi}^* = (\mathbf{I} - \mathbf{\Phi}_0) \mathbf{\Psi} (\mathbf{I} - \mathbf{\Phi}_0)'$ $PDC_{(\eta_m, \eta_n)} = \frac{\phi_{mn}^*}{\sqrt{\psi_{mm}^* \kappa_{nn} + \phi_{mn}^{*2}}}$
DT VAR \rightarrow gVAR with known Δt	

of GIMME and S-GIMME—are indicators that indicate that a parameter is freed for estimation for all subjects within a group or subgroup; however, this is not a single parameter value which applies to all subjects. Following this, the community detection procedure Walktrap (Pons & Latapy, 2005) is applied to identify subgroups of individuals whose models are most similar to one another. Subgroup-level models are then fitted based on the recovered subgroups, with the constraint that the original group-level paths be estimated. Finally, individual sVAR models are fitted to each subject until some convergence criterion are satisfied (see Gates et al., 2017; Gates et al., 2014, for more information). S-GIMME has been applied to the analysis of fMRI (Gates et al., 2014; Henry et al., 2019) and ecological momentary assessment data (EMA; Lane et al., 2019; Park et al., 2021).

Comparing Approaches

Ultimately, the sVAR and gVAR are different models for capturing lagged and contemporaneous relationships between variables but accomplish this goal in unique ways. Further, additional work has described how parameters of the sVAR and gVAR—as an extension of the VAR model—relate to parameters from CT models some of which we have compiled into Table 1 (Chow et al., 2022; Demeshko et al., 2015a). Specific to the sVAR, modeling of contemporaneous effects makes use of directed associations in Φ_0 . Further, in GIMME, estimation of the sVAR is performed via raw data maximum likelihood, with the raw input data containing the concurrent and lagged time-series in separate columns, and produce estimates that are equivalent to the block-Toeplitz approach with no missing data (Molenaar, 1985; Park et al., 2021).

In contrast, the gVAR models contemporaneous information via the inverse of the residual covariance matrix, **K**, with graphical LASSO regularization (GLASSO; Friedman et al., 2008). As a result, the contemporaneous relations in the gVAR are non-directional and indicate the relationship between two variables after partialing out all other associations. Additionally, estimation of gVAR models also capitalizes on use of the lagged time series as predictors within a penalized (as imposed via the GLASSO) least squares

or maximum likelihood framework. Standard error estimates are not available directly from the GLASSO. Inferences are performed instead by using the GLASSO to shrink (and thus biasing) some of the less important coefficients toward zero, with penalized coefficients that fall below a particular threshold subsequently set to zero. As such, inferences involving the gVAR also suffers from some limitations (Park et al., 2021; Williams & Rast, 2020). Conceptually, these differences yield different interpretations on the same data with respect to bidirectional associations—among others—where the sVAR may be capable of providing bidirectional connections from $x \to y$ and $y \to x$ interpreted as individual regression coefficients. In contrast, the gVAR would show a single, nondirectional connection between the two variables indicating a partial correlation between the two variables. More discussion on the similarities and differences between these models can be found in Park et al. (2021) including discussions on the differences between the optimization criterion and possible.

The scgVAR and S-GIMME allow for the identification of subgroups and have found success in the past decade (Gates et al., 2017; Gates et al., 2014; Lane et al., 2019; Park et al., 2021; Wright et al., 2019). Aside from performing subgrouping identification based on alternative variations of the VAR model (the gVAR and SVAR models, respectively), other differences exist between the two approaches (see Epskamp, Waldorp, et al., 2018). For instance, unlike S-GIMME, the scgVAR does not constrain group- or subgroup-level paths to be estimated for all individuals. Moreover, the scgVAR determines edge eligibility by use of the LASSO algorithm whereas S-GIMME makes use of an iterative modification index search.

Despite their differences, both the gVAR and sVAR are simply discrete-time variations of the same CT VAR model (Chow et al., 2022; Demeshko et al., 2015b). One common finding across both approaches is that-in most empirical applications-the networks discovered by these approaches tend to discover mainly contemporaneous effects; that is, most effects tend to occur faster than the lag-1 sampling rate (Wright et al., 2019). This consistent finding may be caused by the empirical sampling rate being significantly slower than the true dynamics or due to omitted common causes which have different lagged influences on the observed variables. Focusing on the former, it is unclear to what extent the performance of these approaches varies when the same CT model is used to generate data and subgroup differences under different time intervals, strengths of coefficients in the drift matrix in Equation 1, and magnitudes of subgroup differences in drift matrix coefficients. These factors have direct implications on the relative distribution of the lagged and contemporaneous effects captured by the two approaches and thus, their relative performances. We conduct a Monte Carlo simulation study to address two specific questions: (1) how well do discrete-time approaches identify subgroup differences in continuous processes across Δt and effect size conditions? and (2) Do differences in Δt and effect size relate to differences in the quality of parameter estimates when using discrete-time approaches on continuous processes?

Simulation Study

In empirical- and simulation-based studies, VAR-based approaches have been used to identify meaningful subgroups with unique structural differences in their discrete-time network dynamics (e.g., Φ_0 , Φ_1 , PDC, or PCC; Bulteel et al., 2016; Henry et al.,

2019; Price et al., 2017). However, the use of intensive longitudinal data is wrought with questions regarding the optimal alignment of time-scales and sampling rates (Ram & Diehl, 2014; Ryan & Hamaker, 2022). For example, these issues arise in studies of daily affect (Wright et al., 2019) where emotions unfold and influence each other faster than data are typically collected and fMRI where neuronal activity occurs significantly faster than the imaging rate (James et al., 2019).

To address these questions, we simulated 2 subgroups of individuals of sample size $N_{total}=50~(n_{g1}=25;n_{g2}=25)$ using a 4-variate Ornstein-Uhlenbeck (OU) model at a temporal resolution of 0.1 units (see Oravecz & Tuerlinckx, 2011). Notably, the interpretation of this temporal resolution depends on the underlying timescale of the process being measured such that 0.1 units could stand for 0.1 seconds or 0.1 weeks, based on the metric for quantifying elapsed time used by the researcher. For example, a $\Delta t=1$ could correspond to a single day and the various values of Δt would then scale in relation to that with $\Delta t=0.1$ relating to assessments every 2.4-hours, $\Delta t=0.5$ relating to assessments every 12-hours, and a $\Delta t=10.0$ being equivalent to an assessment every 10-days. The temporal resolution was held constant across all subjects. The OU model is considered the continuous-time analogue for the discrete-time VAR(1) and is presented in Equation 8 as a special case of Equation 1.

$$d\eta(t) = \mathbf{B}[\mu - \eta(t)] dt + \mathbf{G}d\mathbf{W}(t)$$
(8)

here, **A** in Equation 1 is represented as $-\mathbf{B}$ and $\mathbf{b} = \mathbf{B}\mu$, where **B** is the drift matrix and μ is a vector of intercepts which characterize the resting states or "home-bases" of the p-variables (Oravecz & Tuerlinckx, 2011). Both subgroups shared four auto-regressive and one cross-process effect ($B_{1,1}$, $B_{2,2}$, $B_{3,3}$, $B_{4,4}$, $B_{3,1}$) and differed on two cross-process effects, one in terms of sign only ($B_{1,2}$), and one in terms of path location ($B_{2,4}$ in subgroup 1 and $B_{4,3}$ in subgroup 2).

We examined the influence of effect size, specifically, separation between the two subgroups in drift matrix coefficients under a small and large effect size conditions, with drift matrices: \mathbf{B}_{g1} and \mathbf{B}_{g2} .

$$\mathbf{B_{g1}} = \begin{bmatrix} 0.50 & \sigma & 0.00 & 0.00 \\ 0.00 & 0.50 & 0.00 & -\sigma \\ -\alpha & 0.00 & 0.50 & 0.00 \\ 0.00 & 0.00 & 0.00 & 0.50 \end{bmatrix}, \ \mathbf{B_{g2}} = \begin{bmatrix} 0.50 & -\sigma & 0.00 & 0.00 \\ 0.00 & 0.50 & 0.00 & 0.00 \\ -\alpha & 0.00 & 0.50 & 0.00 \\ 0.00 & 0.00 & -\sigma & 0.50 \end{bmatrix}.$$
(9)

where σ –subgroup specific paths–and α –common paths–took on values of 0.30 or 0.60 in the small and large effect size conditions, respectively. In addition, we repeated the evaluation of effect size using an alternative set of drift coefficients, namely, with cross-process coefficients taking on values of 0.90 and 1.20. This yielded two additional sets of coefficients that mirrored the first evaluation in terms of the separation between subgroups (i.e., "effect size"), but both subgroups' coefficients deviated further from zero and were more prone to show sustained deviations from, or slower return to the system's intercepts. In the other words, this second set of drift coefficients generated dynamics that were closer to the boundary of being unstable (Lütkepohl, 2005). The selection of **B** matrices was to emphasize strong cross-process effects that would vary in their detectability across the tested sampling intervals (Δt) whilst maintaining stationarity. For the simulation study,

we selected the length of T to be T=14 to emulate a 2-week long experiment and T=100 in a manner similar to those seen in the applied time-series literature (e.g., De Vos et al., 2017). These designations—as noted previously—are dependent on the metric of elapsed time determined by the researcher and are used in this study as illustrative examples. As such, if $\Delta t=1.0$ represented a single day then T=14 would be a 2-week long experiment and $\Delta t=0.5$ would be a week long experiment with 2 measures per day. Specific to our data-generation, we simulated over 10,000 time-points based on the continuous OU processes at an interval of $\Delta t=0.1$ -units. We used this Δt and also subsampled the data every 0.5, 1.0, and 10.0 units to emulate subsampling a continuous process at different Δt values. To obtain the target T, we sampled the last 14 or 100 time points of the subsampled time-series to ensure that the effects of any initial (transient) dynamics on the data were discarded.

How Well do Discrete-Time Approaches Identify Subgroups Across Δt and Effect Size Conditions?

For both scgVAR and S-GIMME, subgroup recovery improved as a function of increasing *T* and separation between groups in both the stable and nearly unstable configurations. To accomplish this, we use the Adjusted Rand Index (Hubert & Arabie, 1985). ARIs are calculated as:

$$ARI_{HA} = \frac{\binom{N}{2}(a+d) - [(a+b)(a+c) + (c+d)(b+d)]}{\binom{N}{2}^2 - [(a+b)(a+c) + (c+d)(b+d)]}$$
(10)

where N are number of subjects, a is the number of hits, b is the number of false negative classifications, c is the number of false positives, and d is the number of true negatives. Excellent recovery is $ARI_{HA} > 0.90$, good recovery $ARI_{HA} > 0.80$, moderate recovery is $ARI_{HA} > 0.65$, and values below $ARI_{HA} = 0.65$ are poor (Lane et al., 2019; Steinley, 2004). Notably, reasonable subgroup recovery could be accomplished with limited time points (i.e., T = 14) when Δt was large (e.g., $\Delta t = 10$), with larger separation between subgroups, and strong coefficient strengths (Figure 2). The scgVAR tended to outperform S-GIMME with regard to subgrouping accuracy, especially under less idealized conditions, namely, small T coupled with overly densely spaced repeated measures (small Δt), small separation between subgroups, and weak signal strengths. These differences in recovery may be a result of how S-GIMME was designed to identify subgroups based only on non-zero coefficients during the group search process. Thus, homogeneity in identically zero paths contributed toward subgroup identification in sgcvar but not S-GIMME, thereby reducing the latter's performance in conditions where insufficient non-zero paths were available to distinguish among subgroups.

Conclusion: Discrete-time approaches can identify subgroup differences in continuous processes fairly well; conditional on effect size, Δt , and their interaction. Discrete-time subgrouping approaches perform better in the presence of stronger effect sizes and greater effective distances between the subgroups. Further, larger Δt allowed weaker coefficients to accumulate over the sampling interval and helped the discrete-time algorithms to delineate the subgroups.

Do Differences in Δt and Effect Size Relate to Differences in Bias and Variation in Parameter Estimates?

Overall, both sgcVAR and S-GIMME tended to show underestimation (negative biases) in the values of the parameters in Φ^* and Ψ^* as seen in Figure 3. Biases tended to improve with larger T but with no marked improvement across subgroup separation in the weak and strong drift coefficient configurations. Inspection of the relative biases (rBiases) helped to highlight that scgVAR tended to perform more accurately at small configurations of Δt while S-GIMME struggled, producing substantially larger rBiases especially in situations where the true values of the coefficients (e.g., in some Φ^* elements) were close to zero. In addition, given that S-GIMME by design disregarded identically zero paths as a source of subgroup homogeneity, S-GIMME tended to fix more of the nearzero Φ^* elements to zero than did scgVAR, fix the weak AR paths to 0.00 while scgVAR would estimate some parameters effectively reducing the rBiases. As Δt and subgroup separation increased, rBias for both S-GIMME and scgVAR stayed relatively low. Finally, as $\Delta t = 10$, the rBiases in Φ^* became very poor again. This is due to the fact that the parameters in Φ^* became incredibly small once again and thus more difficult to detect for both algorithms.

Evaluation of the RMSEs indicated that even though only negligible differences in biases were observed for the two approaches for the values in Φ^* under more idealized conditions, S-GIMME tended to yield notably larger RMSEs for Φ^* but conversely, *smaller* RMSEs for values in Ψ^* under $\Delta t = 10$. These points are highlighted in Figure 4. This suggested that the sVAR formulation assumed within the S-GIMME framework in which some contemporaneous covariations among the processes are parameterized into the matrix of contemporaneous effects could yield more stable numerical estimation results for values in Ψ^* when Δt is large. In contrast, sgcVAR, based on its current design that counts identically zero paths in Φ^* as a source of subgroup homogeneity, was more sensitive at estimating values in Φ^* accurately and with less variability across Monte Carlo replications (Chow et al., 2022).

Conclusion: Generally, the point-estimates for discrete-time approaches were relatively unbiased in Φ^* across conditions. Additionally, the point-estimates became less biased in Ψ^* across levels of Δt . However, these relations with Δt and effect size was more complex and multi-faceted than the raw plots would suggest. Biases in Φ^* tended to remain consistently low across Δt ; though, for varying reasons across conditions; discussed below. Relatedly, bias in Ψ^* tended to improve with Δt as effects in the process noises were able to accumulate over the progressively larger sampling intervals with lower RM-SEs as well, reflecting less variability in the point-estimates.

Summary of Results

Taken together, the results of these simulations suggest that both methods–S-GIMME and scgVAR–perform relatively well when subgrouping individuals at large $\Delta t \geq 1.0$ conditions irrespective of the effect size or degree of stability in dynamics. That is, by enabling relatively weak effects to accumulate in the Φ^* and Ψ^* matrices over time, differences between subgroups can be more easily differentiated from one another. These

differences can be detected more easily with greater *T* or with a greater degree of separation between the subgroups.

Both methods returned point-estimates with relatively low-levels of bias; however, the origins of these biases—as discussed above—stems from different causes. When Δt is small, the true Φ^* matrices are very weak. Thus, S-GIMME tended to constrain many paths to 0.00 whereas scgVAR would estimate some paths; this was reflected in the differences in the rBiases. With increased Δt , the true Φ^* -matrices become weak once again alongside significantly more prominent covariances in the true residual covariance matrices, Ψ^* , making detection of Φ^* more difficult for both algorithms. Relatedly, RMSEs in Ψ^* decreased with increases in Δt for both models reflecting less bias and less variability in the parameter estimates.

It is important to note that the parameters in Φ^* and Ψ^* are intricately related to one another and appear in the transformations of each other across modeling frameworks (e.g., from CT to SVAR and VAR), biases in one parameter may be offset/compensated through corresponding biases in other parameters. For instance, the sVAR–from which S-GIMME is derived–embeds contemporaneous information into both the Φ^* and Ψ^* matrices when transformed onto the VAR metric; thus, the same errors may manifest across the transformed VAR matrices in different ways within the simulations. Considering that the contemporaneous effects in the sVAR are obtained by constraining the Ψ^* -matrix to be diagonal, contemporaneous covariances may be modeled as contemporaneous effects in the sVAR which would then be embedded into the Φ^* coefficients matrix via backtransformations covered by Gates et al. (2010).

Ultimately, the results suggest that both S-GIMME and the scgVAR are viable methods for identifying heterogeneous subgroups in continuous processes. Notably, with as few as T=14 timepoints, the scgVAR was able to return acceptable subgroup classifications ($ARI \geq 0.75$) under large effect sizes in our stable configurations. These results can be even more meaningful in cases where sampling at faster intervals is costly or otherwise burdensome to subjects.

Discussion

As noted at the opening of this issue, Molenaar's (2004) call for a return of the person to the scientific study of psychology was heard by many in the behavioral sciences. The commensurate rise in the application of N=1 techniques is a clear indication of this revolution. Similarly, the increased adoption of N=1 analyses led to a rise in criticisms regarding the generalizability of such results to new subjects leading to the emergence of idio-thetic methods. These methods attempt to identify nomothetic commonalities among a set of idiographic processes and have been primarily developed for models in discrete-time including S-GIMME and the scgVAR; both of which have been co-developed by Molenaar (Gates et al., 2014; Park et al., 2022).

The current work sheds light on how well methods for subgrouping originally developed in the discrete-time framework perform at identifying subgroups when the data-generating models are based in continuous-time across a range of discrete sampling intervals. Simulation results indicated that both scgVAR and GIMME performed well in recovering the true subgroup structure with $\Delta t \geq 1.0$ with some promising results when

T was as small as T=14. These results generally fall in line with observations in empirical applications (e.g., Wright et al., 2019) which found that effects in these models tended to be contemporaneous; highlighting that effects were typically occurring faster than the sampling rate. Our work extends this observation to simulated data and suggest that the emergence contemporaneous effects are directly related to Δt as has also been illustrated by Chow et al. (2022) and Demeshko et al. (2015a). In practice, dense measurement intervals (i.e., small Δt) may only be viable with some reduction in T to keep participant burden manageable. Our results indicated that good recovery of subgroup membership and dynamics within the context of dynamic network analysis is contingent on thoughtful consideration of choices for Δt and T.

Even though fitting models in continuous-time circumvents many issues in the discrete-time context, they still represent a vast minority of empirical applications. Further, many if not all, methods for identifying homogeneous clusters of individuals in dynamics are are based in discrete-time. Our work demonstrates that–in instances where fitting continuous-time models are difficult or impractical–subgrouping with the scgVAR or S-GIMME approaches may be useful for identifying meaningful differences between subgroups across a range of $\Delta t'$ s for continuous processes of various strengths.

Limitations

Our study had several limitations than can be addressed in future work. In our simulations measured related to the quality of estimates were excluded due to the relative complexity of transforming the standard errors of S-GIMME back to the standard VAR and the general lack of standard errors produced by the LASSO regularized scgVAR. These issues may be overcome by application of the delta method and bootstrapping methods; however, due to time constraints, these avenues were not pursued. Another limitation was the size of our simulated network. Dynamic network applications typically contain more than four variables. Such larger networks sizes render it difficult to understand the nature and long-run stability (as T approaches ∞) of the dynamic processes of interest in their canonical form for both DT and CT frameworks. Further investigation into the types of dynamics characterizing dynamic networks, the need to include higher-order lags (or alternatively, higher differential order in the CT framework), and properties of the subgrouping methods under diverse types of observed variables is warranted. Further, the DT subgrouping approaches could be compared against clustering approaches developed in the CT framework; however, there currently are not many tools readily available for these methods (e.g., Liu et al., 2020). With these considerations in mind future work will consider applying the scgVAR and S-GIMME subgrouping algorithms to recent extensions capable of fitting sparse VAR models in high-dimensions with both group and individual features (multi-VAR; Fisher et al., 2022).

References

- Arnold, L. (1974). *Stochastic differential equations*. Wiley. https://doi.org/10.1002/zamm. 19770570413
- Beck, E. D., & Jackson, J. J. (2020). Consistency and change in idiographic personality: A longitudinal esm network study. *Journal of Personality and Social Psychology*, 118(5), 1080.
- Bringmann, L. F., Ferrer, E., Hamaker, E. L., Borsboom, D., & Tuerlinckx, F. (2018). Modeling Nonstationary Emotion Dynamics in Dyads using a Time-Varying Vector-Autoregressive Model. *Multivariate Behavioral Research*, 3171, 1–22. https://doi.org/10.1080/00273171.2018.1439722
- Bulteel, K., Tuerlinckx, F., Brose, A., & Ceulemans, E. (2016). Clustering vector autoregressive models: Capturing qualitative differences in within-person dynamics. *Frontiers in Psychology*, 7, 1540.
- Chow, S., Losardo, D., Park, J., & Molenaar, P. (2022). Continuous-time dynamic models: Connections to structural equation models and other discrete-time models. *Structural equation modeling: Concepts, issues, and applications. Guilford.*
- De Vos, S., Wardenaar, K. J., Bos, E. H., Wit, E. C., Bouwmans, M. E., & De Jonge, P. (2017). An investigation of emotion dynamics in major depressive disorder patients and healthy persons using sparse longitudinal networks. *PLoS One*, 12(6), e0178586.
- Demeshko, M., Washio, T., Kawahara, Y., & Pepyolyshev, Y. (2015a). A novel continuous and structural var modeling approach and its application to reactor noise analysis. *ACM Transactions on Intelligent Systems and Technology (TIST)*, 7(2), 1–22.
- Demeshko, M., Washio, T., Kawahara, Y., & Pepyolyshev, Y. (2015b). A novel continuous and structural var modeling approach and its application to reactor noise analysis. *ACM Transactions on Intelligent Systems and Technology*, 7, 1–22. https://doi.org/10.1145/2710025
- Epskamp, S., van Borkulo, C. D., van der Veen, D. C., Servaas, M. N., Isvoranu, A.-M., Riese, H., & Cramer, A. O. (2018). Personalized network modeling in psychopathology: The importance of contemporaneous and temporal connections. *Clinical Psychological Science*, 6(3), 416–427.
- Epskamp, S., Waldorp, L. J., Mõttus, R., & Borsboom, D. (2018). The gaussian graphical model in cross-sectional and time-series data. *Multivariate Behavioral Research*, 53(4), 453–480.
- Fisher, Z. F., Kim, Y., Fredrickson, B. L., & Pipiras, V. (2022). Penalized estimation and forecasting of multiple subject intensive longitudinal data. *Psychometrika*, 1–29.
- Friedman, J., Hastie, T., & Tibshirani, R. (2008). Sparse inverse covariance estimation with the graphical lasso. *Biostatistics*, *9*(3), 432–441.
- Gates, K. M., Lane, S. T., Varangis, E., Giovanello, K., & Guiskewicz, K. (2017). Unsupervised classification during time-series model building. *Multivariate behavioral research*, 52(2), 129–148.
- Gates, K. M., & Molenaar, P. C. (2012). Group search algorithm recovers effective connectivity maps for individuals in homogeneous and heterogeneous samples. *NeuroImage*, 63(1), 310–319.

- Gates, K. M., Molenaar, P. C., Hillary, F. G., Ram, N., & Rovine, M. J. (2010). Automatic search for fmri connectivity mapping: An alternative to granger causality testing using formal equivalences among sem path modeling, var, and unified sem. *NeuroImage*, 50(3), 1118–1125.
- Gates, K. M., Molenaar, P. C., Iyer, S. P., Nigg, J. T., & Fair, D. A. (2014). Organizing heterogeneous samples using community detection of gimme-derived resting state functional networks. *PloS one*, 9(3), e91322.
- Gollob, H. F., & Reichardt, C. S. (1987). Taking account of time lags in causal models. *Child development*, 80–92.
- Henry, T. R., Feczko, E., Cordova, M., Earl, E., Williams, S., Nigg, J. T., Fair, D. A., & Gates, K. M. (2019). Comparing directed functional connectivity between groups with confirmatory subgrouping gimme. *NeuroImage*, 188, 642–653.
- Horgan, J. (1992). The new challenges. Scientific American, 267(6), 16–23.
- Hubert, L., & Arabie, P. (1985). Comparing partitions. *Journal of classification*, 2(1), 193–218.
- James, O., Park, H., & Kim, S.-G. (2019). Impact of sampling rate on statistical significance for single subject fmri connectivity analysis. *Human brain mapping*, 40(11), 3321–3337.
- Lane, S. T., Gates, K. M., Pike, H. K., Beltz, A. M., & Wright, A. G. (2019). Uncovering general, shared, and unique temporal patterns in ambulatory assessment data. *Psychological Methods*, 24(1), 54.
- Liu, S., Ou, L., & Ferrer, E. (2020). Dynamic mixture modeling with dynr. *Multivariate Behavioral Research*, 1–15.
- Lütkepohl, H. (2005). *New introduction to multiple time series analysis*. Springer Science & Business Media.
- Molenaar, P. C. M. (1985). A dynamic factor model for the analysis of multivariate time series. *Psychometrika*, 50, 181–202.
- Molenaar, P. C. (2004). A manifesto on psychology as idiographic science: Bringing the person back into scientific psychology, this time forever. *Measurement*, 2(4), 201–218.
- Molenaar, P. C. (2017). Equivalent dynamic models. *Multivariate behavioral research*, 52(2), 242–258.
- Oravecz, Z., & Tuerlinckx, F. (2011). The linear mixed model and the hierarchical ornstein—uhlenbeck model: Some equivalences and differences. *British Journal of Mathematical and Statistical Psychology*, 64(1), 134–160.
- Park, J. J., Chow, S.-M., Epskamp, S., & Molenaar, P. (2022). Subgrouping with chain graphical var models.
- Park, J. J., Chow, S.-M., Fisher, Z. F., & Molenaar, P. C. (2021). Affect and personality: Ramifications of modeling (non-) directionality in dynamic network models. *European Journal of Psychological Assessment*, 36(6), 1009–1023.
- Pons, P., & Latapy, M. (2005). Computing communities in large networks using random walks. *International symposium on computer and information sciences*, 284–293.
- Price, R. B., Lane, S., Gates, K., Kraynak, T. E., Horner, M. S., Thase, M. E., & Siegle, G. J. (2017). Parsing heterogeneity in the brain connectivity of depressed and healthy adults during positive mood. *Biological psychiatry*, 81(4), 347–357.

- Ram, N., & Diehl, M. (2014). Multiple-time-scale design and analysis: Pushing toward real-time modeling of complex developmental processes. In *Handbook of intraindividual variability across the life span* (pp. 328–343). Routledge.
- Rothman, A. J., Levina, E., & Zhu, J. (2010). Sparse multivariate regression with covariance estimation. *Journal of Computational and Graphical Statistics*, 19(4), 947–962.
- Ryan, O., & Hamaker, E. L. (2022). Time to intervene: A continuous-time approach to network analysis and centrality. *Psychometrika*, 87(1), 214–252.
- Steinley, D. (2004). Properties of the hubert-arable adjusted rand index. *Psychological methods*, *9*(3), 386.
- Tibshirani, R. (1996). Regression shrinkage and selection via the lasso. *Journal of the Royal Statistical Society: Series B (Methodological)*, 58(1), 267–288.
- Voelkle, M. C., Oud, J. H., Davidov, E., & Schmidt, P. (2012). An sem approach to continuous time modeling of panel data: Relating authoritarianism and anomia. *Psychological methods*, 17(2), 176.
- Wild, B., Eichler, M., Friederich, H.-C., Hartmann, M., Zipfel, S., & Herzog, W. (2010). A graphical vector autoregressive modelling approach to the analysis of electronic diary data. *BMC medical research methodology*, 10(1), 28.
- Williams, D. R., & Rast, P. (2020). Back to the basics: Rethinking partial correlation network methodology. *British Journal of Mathematical and Statistical Psychology*, 73(2), 187–212.
- Wright, A. G., Gates, K. M., Arizmendi, C., Lane, S. T., Woods, W. C., & Edershile, E. A. (2019). Focusing personality assessment on the person: Modeling general, shared, and person specific processes in personality and psychopathology. *Psychological Assessment*, 31(4), 502.

17

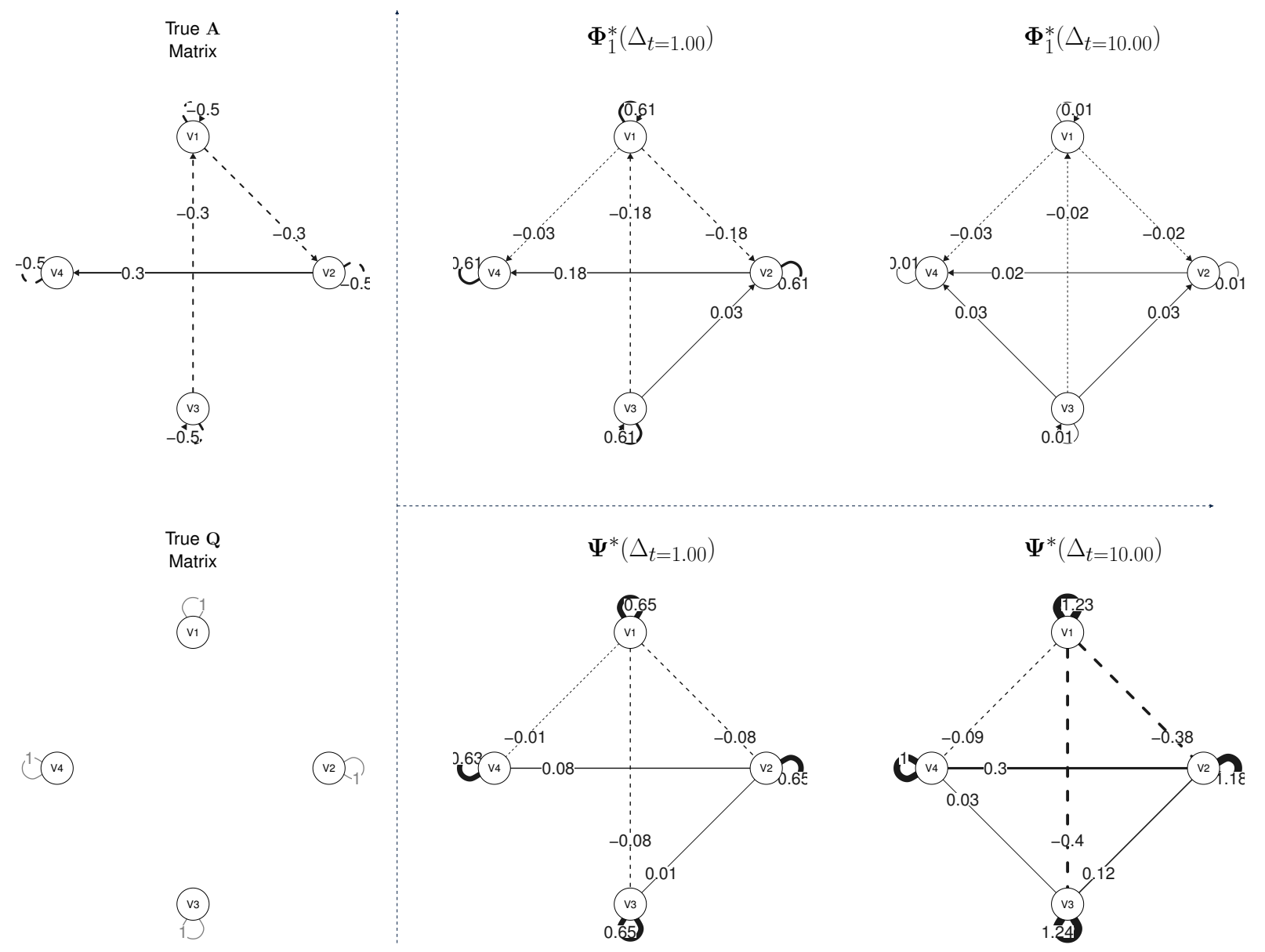


Figure 1. Relating the True CT VAR (**A** and **Q**) to the DT VAR at a $\Delta_t = 1$ ($\Phi_1^*(\Delta_{t=1})$) and $\Psi^*(\Delta_{t=1})$) and $\Delta_t = 10$ ($\Phi_1^*(\Delta_{t=10})$) and $\Psi^*(\Delta_{t=10})$). Solid lines indicate positive coefficients while dashed lines indicate negative coefficients. Notably, paths in **A** become weaker as Δ_t increases but manifest as covariances in the Ψ^* matrices.

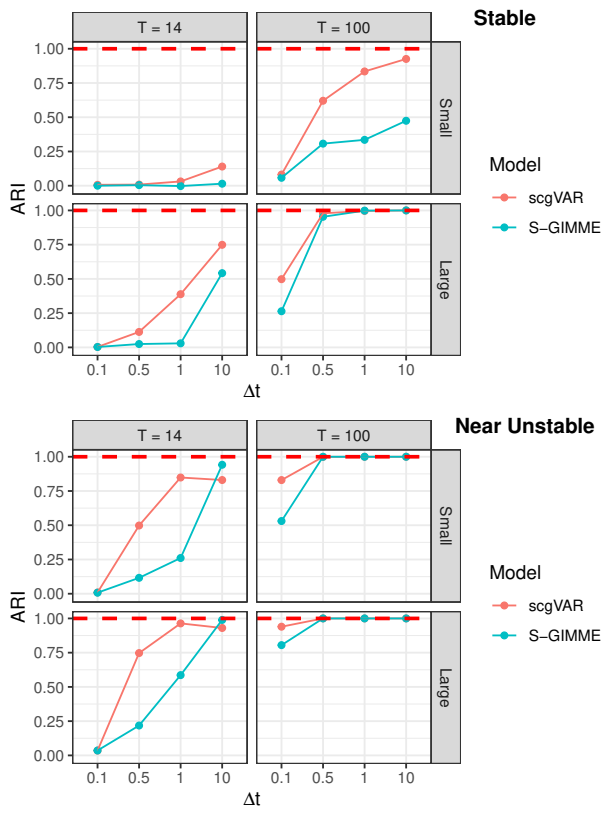
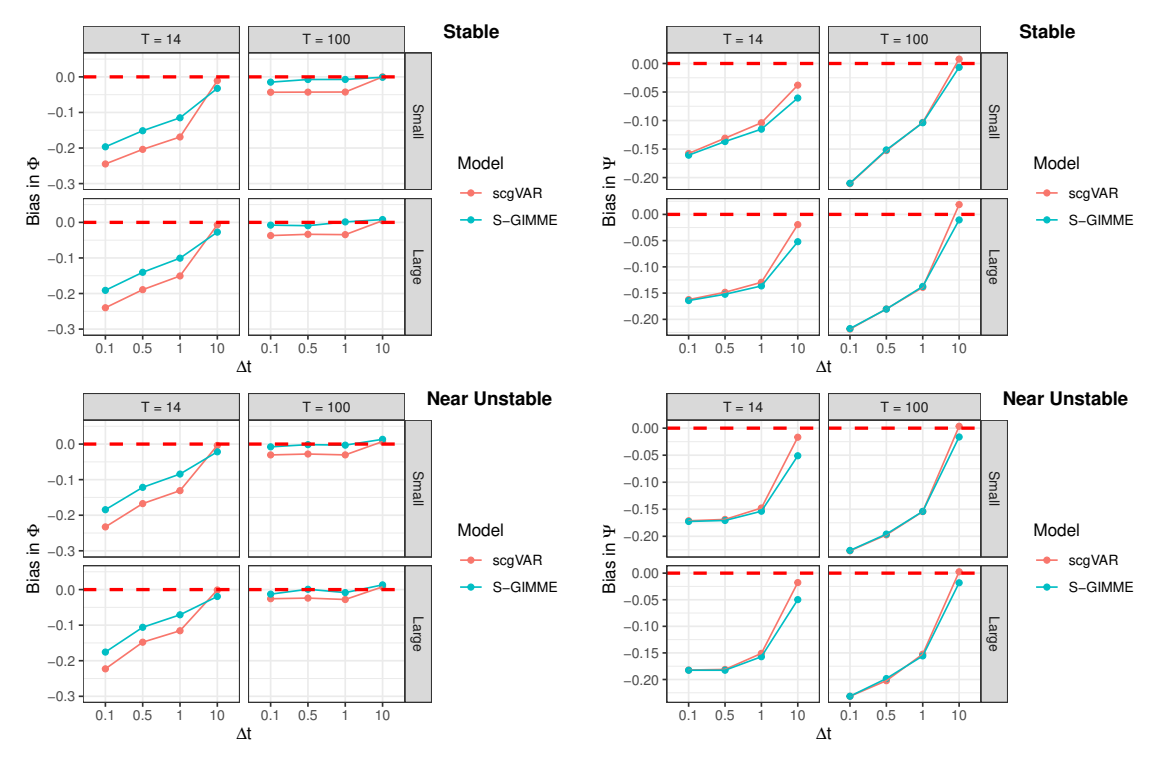
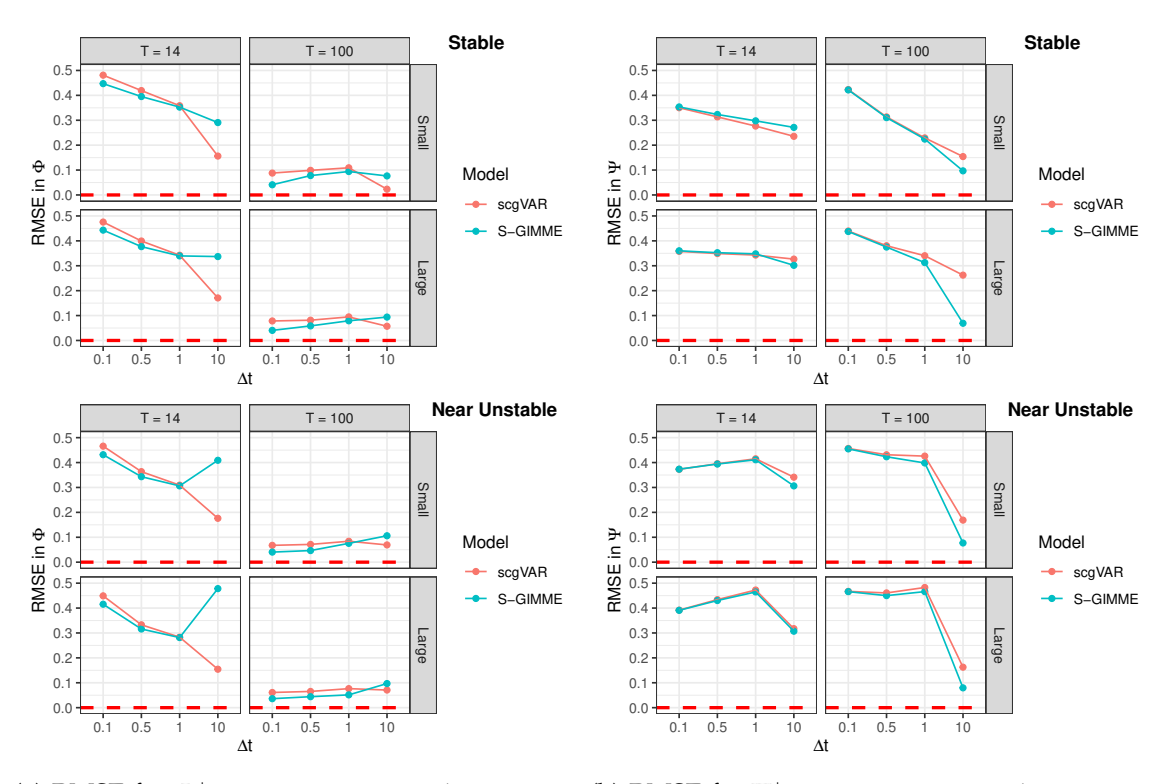


Figure 2. Average ARIs across Δt Conditions relative to the presence of individual differences. Subgroup membership is relatively poor across small T configurations across Δt but improves as Δt becomes large. Similarly, accuracy improves as T increases from 14 to 100.



(a) Biases for Φ^* -parameters across Δt (b) Biases for Ψ^* -parameters across Δt Figure 3. Biases of non-zero parameters for both S-GIMME and the scgVAR when transformed to the VAR metric. Biases were calculated as: $\mathrm{Bias}(\theta) = \frac{1}{H} \sum_{h=1}^{H} \left(\hat{\theta}_h - \theta\right)$. θ and $\hat{\theta}$ represent the parameters and their estimates, H is the number of simulations.



(a) RMSE for Φ^* -parameters across Δt (b) RMSE for Ψ^* -parameters across Δt Figure 4. RMSE's of non-zero parameters for both S-GIMME and the scgVAR when transformed onto the VAR metric. RMSEs were calculated as: $RMSE(\theta) = \sqrt{\frac{1}{H}\sum_{h=1}^{H}(\hat{\theta}_h - \theta)^2}$